AGU PUBLICATIONS

Geophysical Research Letters

RESEARCH LETTER
10.1002/2015GL066049

Key Points:
- Arctic snow depths show distinct distributions on multiyear and first-year ice
- Model biases in summer snow depth affects model spring snow depth biases
- The trend in snow depth in first half of 21st century is mainly a result of shift from MY to FY ice

Supporting Information:
- Figures S1–S4

Correspondence to:
E. Blanchard-Wrigglesworth,
ed@atmos.washington.edu

Citation:
Blanchard-Wrigglesworth, E., S. L. Farrell, T. Newman, and C. M. Bitz (2015), Snow cover on Arctic sea ice in observations and an Earth System Model, *Geophys. Res. Lett.*, *42*, 10,342–10,348, doi:10.1002/2015GL066049.

Received 2 SEP 2015
Accepted 21 NOV 2015
Accepted article online 1 DEC 2015
Published online 14 DEC 2015

©2015. American Geophysical Union. All Rights Reserved.

Snow cover on Arctic sea ice in observations and an Earth System Model

E. Blanchard-Wrigglesworth[1], S. L. Farrell[2], T. Newman[2], and C. M. Bitz[1]

[1]Department of Atmospheric Sciences, University of Washington, Seattle, Washington, USA, [2]Earth System Science Interdisciplinary Center, University of Maryland, College Park, Maryland, USA

Abstract Spring snow depth on Arctic sea ice is assessed in observations and an Earth System Model. In both, snow depth is mainly driven by the ice type on which the snow lies. Snow depths on multiyear ice are approximately double snow depths on first-year ice. In the model spring snow depths are greater on multiyear ice compared to first-year ice primarily because multiyear ice begins to accumulate snow earlier in the fall but also due to snow cover survival through the summer on multiyear ice. The model simulates a decline in spring snow depth driven mainly by a transition from a multiyear to first-year ice regime throughout the Arctic. Agreement in the loss of multiyear ice in the model with estimates from observations suggests that declining snow depths in observations mainly result from the loss of multiyear sea ice.

1. Introduction

Snow on sea ice is a key component of the Arctic climate system. During the summer, it slows down ice melt, while its higher-than-ice albedo reflects a larger amount of incoming solar radiation than bare sea ice or open ocean [e.g., *Maykut and Untersteiner*, 1971]. During the winter, it acts as an insulator and reduces the heat loss from the ice/ocean to the atmosphere, thereby slowing down sea ice growth. Snow also impacts melt pond formation [*Polashenski et al.*, 2012], which itself plays a role in the energy budget of the Arctic and summer melt of the ice pack. Historically, direct measurements of snow on sea ice have been sparse in space and time. The widely used snow climatology of *Warren et al.* [1999], hereafter W99, was mainly derived from measurements collected at drifting Soviet stations on multiyear ice (MYI) over the period 1954–1991. Since then the Arctic cryosphere has undergone significant changes, highlighted by a rapid decline in sea ice extent and thickness [e.g., *Serreze et al.*, 2007; *Kwok and Rothrock*, 2009], a loss of MYI in favor of first-year ice (FYI, e.g., *Maslanik et al.* [2011], and a decline in spring snow depth [*Webster et al.*, 2014]).

Since 2009, NASA's ongoing Operation IceBridge has flown yearly transoceanic airborne surveys of Arctic sea ice properties between mid-March and the end of April. IceBridge measures snow depth using a frequency-modulated continuous-wave (FMCW) snow radar while simultaneously identifying MYI and FYI types owing to their distinctive surface roughness. *Kurtz and Farrell* [2011] analyzed snow radar data collected in 2009 and found significantly different snow depth over MYI and FYI, with mean depths of 31 cm and 16 cm, respectively. The measured depths represent snow accumulation since the previous summer, as snow generally completely melts every summer over all ice types [e.g., *Lindsay*, 1998].

Meanwhile, *Hezel et al.* [2012] showed snow depths in the across model ensemble mean of twentieth century integrations archived by the Coupled Model Intercomparison Project 5 (CMIP5) agreed well with the W99 climatology and IceBridge data. However, CMIP5 models do not track sea ice age and therefore that study could not assess the relationship between sea ice age and snow depth in the models—note that a model could replicate the observed mean snow depth along an IceBridge transect but have biased MYI/FYI areas and snow depth distributions on each ice type. *Hezel et al.* [2012] also found that each model had a decline in April snow depth over Arctic sea ice in 21st century greenhouse warming scenarios, despite an increase in winter snowfall. The chief cause for the decline in snow depth is a loss of sea ice area in autumn and early winter, which shortens the accumulation season. *Hezel et al.* [2012] speculated that this same mechanism explains the spatial distribution of snow in observations with less snow on FYI compared to MYI because the accumulation season is shorter on FYI, while *Webster et al.* [2014] found spring snow depth trends to be correlated with freeze-up dates in observations. However, this study also found a loss in spring snow depth over regions of MYI north of the Canadian Archipelago and Greenland, where changing freeze-up dates are unlikely to play a role.

In this study we employ an Earth System Model (ESM) that diagnoses FYI and MYI types [*Armour et al.*, 2011; *Jahn et al.*, 2012] to evaluate the snow depth to ice type relationship in detail compared with IceBridge observations. We investigate the physical processes that give rise to the snow depth distribution with respect to ice type and extend our analysis to examine how these relationships evolve in a 21st century greenhouse warming scenario.

2. Data Sets and Methods

We use IceBridge snow depth observations collected in March/April 2011–2012 across both FYI and MYI in the western Arctic Basin, as described in *Newman et al.* [2014]. Snow depths were extracted from frequency-modulated continuous-wave (FMCW) radar echograms using a novel wavelet retrieval technique and topographic filtering and have been validated via comparison with measurements collected in situ across a range of ice types in the Beaufort Sea. The observations represent snow accumulation on relatively level ice including sastrugi, with an associated average accuracy across basin scales of 6 cm [*Newman et al.*, 2014]. *Kwok and Haas* [2015] found that the original IceBridge FMCW snow radar data contained artifacts caused by side lobes, which could impact snow depth estimates. *Newman et al.* [2014] mitigate against these impacts in their wavelet retrieval approach to identify the air/snow interface in radar echograms, arguably producing the best quality snow depth estimates from IceBridge observations to date. We have applied a 1 km along-track arithmetic averaging scheme to the airborne snow depths to account for gaps in the data and reduce small-scale along-track variability and remaining measurement noise.

We use output from the Large Ensemble (LE) of the Community Earth System Model version 1 with the Community Atmosphere Model version 5 (CESM1-CAM5 [*Kay et al.*, 2014]). The sea ice component in this model is the Los Alamos Sea Ice Model (CICE) version 4 [*Hunke et al.*, 2010] and is considered a leader among ESMs (see *Blazey et al.* [2013] for a description of how snow on sea ice is treated in CICE). The LE consists of 30 ensemble members forced with historical greenhouse gases and aerosol emissions from 1920–2005 and the 21st century representative concentration pathway 8.5 (RCP8.5) scenario through 2100. The RCP8.5 is a high-emission scenario with direct radiative forcing reaching 8.5 W m^{-2} (1370 ppm CO_2 equivalent) in 2100. The initial conditions in 1920 are perturbed slightly across the ensemble. We begin our analysis in 1925 when practically all memory of the initial conditions in the sea ice is lost and the spread among the ensemble at a particular time is a measure of natural variability (not shown). The model has a FYI sea ice tracer that is area conserving and keeps an account of all ice that grows from 15 September in one year to the next, when all FYI is promoted to MYI and the account is reset to zero.

We take advantage of the LE to obtain an accurate estimate of the model's true mean and natural variability along the IceBridge flight tracks and dates (the "IceBridge domain," Figure S1) by using all 30 ensemble members. While the grid cell size in the model (about 25–30 km) is larger than the IceBridge 1 km averaged values, sampling from all 30 ensemble members results in a comparable population size for observations and model. The snow depth autocorrelation in observations (model) is $r = 0.1$ ($r = 0.5$), resulting in a higher number of degrees of freedom in the observations, yet both data sets have a large number of degrees of freedom (~40,000 in observations and ~25,000 in the model). We calculate pan-Arctic values by calculating area-weighted means north of 70° over sea ice. In CESM, each grid cell has one value for snow depth per ice thickness category, and thus, we cannot distinguish snow depths across ice types within a single grid cell. We classify grid cells as MYI (FYI) if their multiyear (first-year) ice concentration is greater (lower) than 50%. While the 50% limit is arbitrary, it is suitable since we find Arctic sea ice within a grid cell is either predominantly FYI or MYI (not shown).

3. Results

We begin by comparing spring snow depths along the IceBridge domain in CESM with IceBridge observations, as shown in Figure 1 and Table 1. Both have distinct snow depths distributions on FYI and MYI (Figure 1). In CESM, the mean snow depth on FYI is 25 cm with a mode of 21 cm, while in observations the mean snow depth on FYI is 20 cm with a mode of 17 cm. The mean snow depth on MYI in CESM is 50 cm with a mode of 36 cm, while the observations have a mean snow depth on MYI of 32 cm with a mode of 30 cm. There are more data over MYI than FYI for both CESM and IceBridge, since most sea ice in the IceBridge domain is MYI. In CESM, on MYI snow depths under 10 cm never occur. In the IceBridge data set of *Newman et al.* [2014], no snow depths under 10 cm are recorded owing to a necessary cutoff used in the wavelet retrieval technique that accounts for

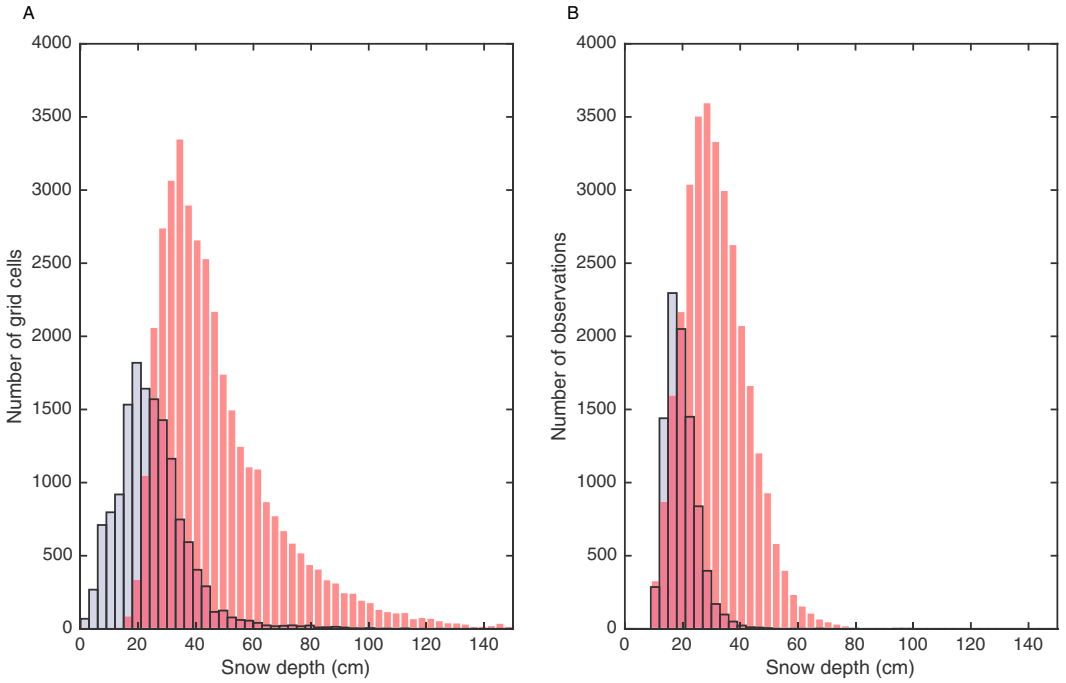

Figure 1. Histogram of spring snow depth on FYI (light blue bars) and MYI (light red bars) in (a) CESM and (b) IceBridge. The grid cells are daily means in CESM that are sampled along the IceBridge domain in space and time across all 30 ensemble members.

current radar deficiencies, including side lobe artifacts, that inhibit sampling small snow depths. Snow depths are more variable over both ice types in CESM relative to IceBridge, with a standard deviation of 30 cm over MYI and 12 cm over FYI in CESM compared to 11 cm over MYI and 6 cm over FYI in IceBridge. This is illustrated by the long tails of the CESM snow depth distributions in Figure 1, particularly for snow depths over MYI.

Despite these differences, we are encouraged by the agreement between the modeled and observed spring snow depths on Arctic sea ice, in particular the distinct distributions over FYI and MYI, and the form of these distributions. In both CESM and IceBridge, the differences between mean snow depth over FYI and MYI are statistically significant at the 99% level. Nevertheless, it is also clear that modeled snow depth variability is significantly greater than observed snow depth variability and the tails of the distributions are longer, leading to a larger mean snow depth, particularly over MYI (Figure S2). The differences in mean snow depth and variability between CESM and IceBridge are also evident when considering individual LE members and IceBridge data years (Figure S3). The differences in mean snow depth over MYI and snow depth variability over MYI and FYI between CESM and IceBridge are statistically significant at the 99% level.

We consider how the snow depth characteristics compare over the IceBridge and pan-Arctic domains in CESM (Table 1) for the same spring dates. Mean snow depth on FYI (MYI) is 25 cm (50 cm) over the IceBridge domain, while it is 23 cm (38 cm) across the Arctic Basin. Variability of snow depth on FYI is comparable over the IceBridge domain and the pan-Arctic domain (standard deviations of 12 cm and 13 cm, respectively),

Table 1. Mean, Mode, and Standard Deviations of Snow Depth Over the IceBridge and Pan-Arctic Domains

Variable		IceBridge Observations	CESM (IceBridge Domain & Dates)	CESM (Pan-Arctic Domain & IceBridge Dates)
Snow on FYI	Mean	20 cm	25 cm	23 cm
	Standard deviation	6 cm	12 cm	13 cm
	Mode	17 cm	21 cm	21 cm
Snow on MYI	Mean	32 cm	50 cm	38 cm
	Standard deviation	11 cm	30 cm	21 cm
	Mode	30 cm	36 cm	31 cm

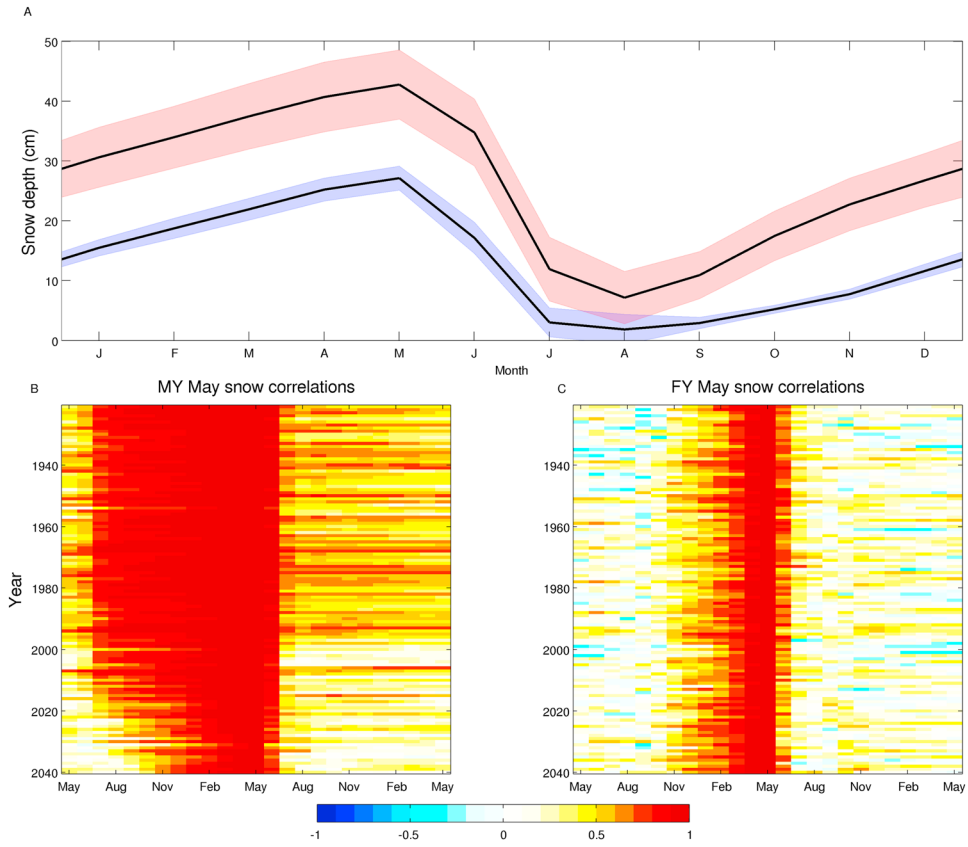

Figure 2. (a) Seasonal cycle of snow depth in CESM. Mean monthly snow depth (in cm) on MYI (light red) and FYI (light blue) sea ice types for 2009–2013. The shaded areas represent the ±1 standard deviation about the mean. (b and c) Lagged correlations of snow depth anomalies in CESM in May (at the time of seasonal maximum) with snow depth anomalies in the months preceding and following May (lags −13 to +13 months) over MYI (Figure 2b) and FYI (Figure 2c) across the large ensemble.

while variability of snow depth on MYI is greater in the IceBridge domain relative to the pan-Arctic domain (standard deviations of 30 cm and 21 cm, respectively). These differences in snow depth on MYI between the IceBridge and pan-Arctic domains can be understood in the context of the mean state of Arctic sea ice. Ice tends to be thickest and snow deepest in the western Arctic and north of the Canadian Arctic Archipelago and Greenland, where the IceBridge domain is located (Figure S1). Nevertheless, the distinct distribution of snow depth by ice type holds over most of the Arctic. Indeed, the controlling influence that ice type exerts on snow depth is further illustrated by the fact that the fraction of ice type within the Arctic Basin explains a significant fraction of the variability in mean April pan-Arctic snow depth in CESM. During the period 1925–2040 (before most MYI is lost), ice type fraction explains on average about 35% of the spread in snow depth each year across the LE members (see Figure S4).

Next, we consider the origin of the different spring snow depths on FYI and MYI sea ice. If the ''autumn platform'' mechanism [*Hezel et al.*, 2012] dominates, we would expect the seasonal amplitude of snow depth on MYI and FYI to be significantly different: from a common initial starting point at the end of summer, snowfall on MYI would accumulate while snow accumulation on FYI would be impeded until the formation of FYI sea ice, and greater snow depth on MYI would also result in a larger seasonal cycle of snow depth on MYI. Figure 2a shows the monthly ensemble mean snow depth on MYI and FYI over the period 2009–2013 in the LE. The seasonal cycle amplitude for snow on FYI is 25 cm, while for snow on MYI it is 35 cm. However, this difference of 10 cm cannot account for the total difference in snow depth across ice types in spring, at the time of the annual maximum, which is 16 cm (annual maximum snow depth is 43 cm for MYI and 27 cm for FYI). The additional process at play in CESM is the partial survival of snow cover on MYI through the

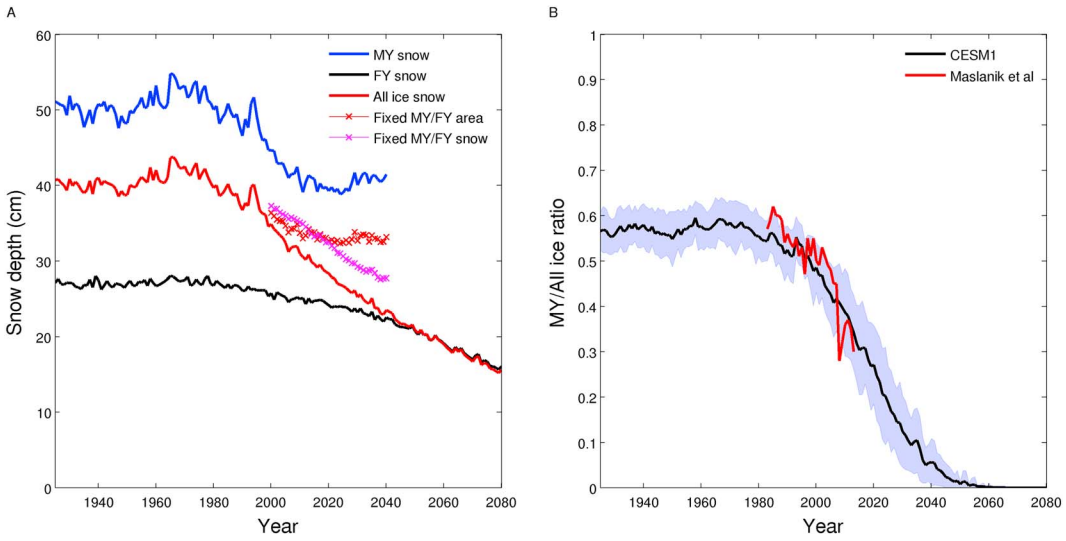

Figure 3. (a) April mean snow depth on MYI (blue), FYI (black), and all ice types (red) for 1925–2080. The red-crossed line represents the April snow depth that would result from keeping the ratios of MYI and FYI area fixed to the 1980–2000 mean but using temporally variable April MYI and FYI snow depths, while the purple-crossed line represents the April snow depth that would result from keeping the April snow depths over MYI and FYI fixed to the 1980–2000 mean but using temporally variable April MYI and FYI areas. MYI snow is only shown until 2040, when most MYI disappears . (b) April ratio of MYI area to all ice types area in CESM (light blue) for 1925–2080 and observational estimates taken from *Maslanik et al.* [2007] (red) for 1983–2013. The shaded area represents the ±1 standard deviation about the mean in CESM.

summer season. Thus, snow on MYI begins to accumulate in the autumn from a deeper starting snow depth than snow on FYI, which starts to accumulate from zero.

As a consequence of the survival in summer of some snow on MYI, snow depths on MYI tend to be much more variable than snow depths on FYI (Figure 2a), as snow depths on MYI not only depend on snowfall during the cold season but also on summer temperatures and snowfall [*Light et al.*, 2015]. Lagged correlations of snow depth (Figures 2b and 2c) indicate that spring snow depths over MYI are strongly correlated with previous summer snow depths (a deep snow cover in summer leads to a deep snow cover in the following spring), whereas spring snow depths over FYI are only correlated with snow depths during the previous winter and more weakly the previous autumn.

Next, we consider trends in April snow depth in the LE. Figure 3a shows that between 2000 and 2040 April snow depths decrease on FYI and MYI, but the decrease is greater for snow depth over all ice, which we take as the area-weighted snow depth over both FYI and MYI. This is explained by the change in ice type regime from an Arctic Basin dominated by MYI in the twentieth century to one dominated by FYI in the 21st century (Figure 3b). Since the mean snow depth on MYI is greater than on FYI, a trend in overall snow depth would take place simply by replacing MYI with FYI, even with no change in snow depth over the individual FYI or MYI types. To illustrate this quantitatively, we calculate the all-ice snow depth in the 2000–2040 period that would result without a change in ice type (by maintaining the MYI/FYI ratio fixed to the 1980–2000 mean) but accounting for the varying snow depth in time over each ice type. This is shown by the red crosses in Figure 3a and amounts to a 2000–2040 trend in snow depth of 0.7 cm/decade. We also calculate the mean snow depth in the 2000–2040 period that would result without a change in snow depth over individual ice types (by maintaining the MYI and FYI snow depths fixed to the 1980–2000 mean) but accounting for the varying ice type areas in time. This is shown by the purple crosses in Figure 3a and amounts to a 2000–2040 trend in snow depth of 2.5 cm/decade. The actual 2000–2040 trend in snow depth is 2.7 cm/decade. Therefore, most of the decrease in spring all-ice snow depth between 2000 and 2040 in CESM is a result of the transition of the ice pack from MYI to FYI, rather than a loss of snow on either MYI or FYI. Beyond 2040, CESM predicts negligible survival of MYI at the end of summer in the Arctic Basin, and thus, all-ice snow trends are dictated by trends of snow on FYI.

While MYI snow depth only has a modest influence on all-ice snow depth as discussed above, it shows an interesting evolution throughout the model simulation—a stable period between 1925 and 1990 is followed

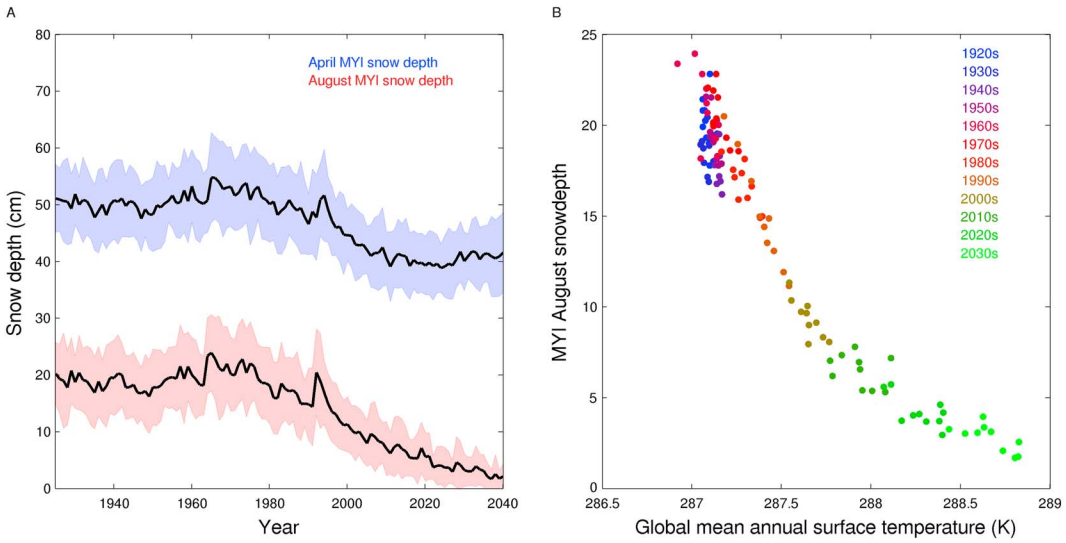

Figure 4. (a) April and August mean snow depth on MYI, 1925–2040. The shaded areas represents the ±1 standard deviation about the mean. (b) Scatterplot of August mean snow depth on MYI and mean global temperatures.

by a period of decline that ends around 2020, after which snow depth remains stable again, despite continuing anthropogenic forcing. In Figure 4a we show both April and August snow depth on MYI in CESM. The period of decline in April snow depth on MYI is contemporary with the loss in August snow depth on MYI, which is a result of enhanced summer snow melt during this period (not shown). Hence, a loss of summer snow results in a decline in spring snow depth over MYI. Interestingly, there is a close, nonlinear relationship between global mean annual temperatures and August snow depth (Figure 4b), and the loss of summer snow between 1990 and 2020 is contemporary with a warming of ~0.8°C in global temperature. Similar relationships exist between August snow depth and Northern Hemisphere or Arctic (north of 70°N) mean annual temperatures (not shown). We discuss the implications of this mechanism further in the discussion below.

4. Discussion and Conclusions

We have shown that a distinct distribution of spring snow depths over MYI and FYI in the Arctic is replicated in both a state-of-the-art ESM and in novel snow depth measurements from airborne instruments. Snow depths over FYI are approximately half of snow depths on MYI. In the model, the primary reason behind this distribution is a greater accumulation of snow on ice during the autumn over MYI, a time when most FYI has not formed yet and is thus unable to accumulate snow. This is reflected in a greater seasonal cycle amplitude of snow depth on MYI. We find, however, that about a third of the difference in spring snow depth between ice types in the model is due to the summer survival of snow cover over MYI that is not possible over FYI (since by definition FYI has formed since September). Although no IceBridge snow depth measurements have yet been collected during the summer period, evidence from other observational data indicates that snow cover does not generally survive through the summer [e.g., *Lindsay*, 1998], and this is also the season with the largest positive bias in snow depth relative to the W99 climatology in an earlier version of CESM [*Blazey et al.*, 2013]. It is thus likely that in observations the main process driving the different distributions of spring snow depth on MYI and FYI is the autumn accumulation of snow on MYI, while the survival of summer snow over MYI in CESM likely contributes to the greater positive bias in mean spring snow depth over MYI (50 cm versus 32 cm) relative to FYI (25 cm versus 20 cm, Table 1). The higher spring snow depth variability in MYI relative to FYI in CESM that results from the survival of the previous summer snow depth is also unlikely to be realistic. However, further summer observations are required to confirm these hypotheses.

We also find that projected future losses in snow depth in the spring are driven primarily by a transition from MYI to FYI in the Arctic. However, the likely biased simulation of summer survival of snow cover in the model poses challenges when assessing this trend. In CESM, a fraction of the loss in spring snow depth over MYI is due to the loss of summer snow over MYI as the Arctic warms in the early 21st century, and this mechanism is unlikely to play a role in observations. To assess the importance of this bias, we plan future simulations with this GCM that correct the bias in summer snow cover over the Arctic.

A second factor that needs to be considered when assessing trends in spring snow depth in observations and CESM is the rate at which FYI replaces MYI in a warming Arctic. Estimates of sea ice age in observations have made it possible to calculate the proportion of MYI and FYI in the Arctic throughout the satellite era [e.g., *Maslanik et al.*, 2007]. These estimates of loss of MYI in observations are in close agreement to the loss of MYI in the GCM (see Figure 3b) during the last three decades. It is worth noting that *Webster et al.* [2014] found observational evidence of a decrease in spring snow depth from 35 $\pm$ 9 cm to 22 $\pm$ 2 cm over the western Arctic, a decline of 37 $\pm$ 29%, between 1954–1991 and 2009–2013. In CESM, mean April snow depth decreases from 41 cm to 31 cm over the same period, a decline of 24%.

It is intriguing that *Webster et al.* [2014] found a reduction in spring snow depth over regions of MYI in observations between the W99 climatology (1954–1991) and the IceBridge data available to them (2009–2013, see, e.g., Figure 8 in that study) despite no changes in accumulation rates or, by definition, freezing dates of MYI. It is possible that the mechanism by which a loss of summer snow leads to a reduction in spring snow over MYI that the CESM simulates may help explain the trend seen in observations by [*Webster et al.*, 2014]. Evidence of August snow cover in W99 (see their Figure 9) and global warming of $\sim$ 0.6°C between the W99 and IceBridge periods is broadly consistent with the CESM values above (if albeit not the timing) and raises the possibility that during cooler periods prior to the W99 climatology, a summer snow cover may have been even more consistent. Unfortunately, no early scientific Arctic expeditions known to us (e.g., the 1893–1896 Norwegian North polar expedition [*Nansen*, 1905]) included systematic snow depth measurements, precluding us from testing this hypothesis further.

Acknowledgments

NASA IceBridge Snow Radar Level-1B Geolocated Radar Echo Strength Profiles (IRSNO1B) data are available at the National Snow and Ice Data Center: http://nsidc.org/data/irsno1b.html and directly from the University of Kansas Center for Remote Sensing of Ice Sheets (CReSIS): https://data.cresis.ku.edu/. The CESM Large Ensemble data are available from the Earth System Grid (http://www.earthsystemgrid.org). The authors thank the IceBridge Teams and the support of the CReSIS for their diligent efforts in gathering and processing the IceBridge snow radar data. This work was supported by NASA grant NNX14AI03G and by the NOAA Ocean Remote Sensing Program. We thank the National Science Foundation and the Department of Energy for supporting the CESM project, which includes the Large Ensemble Community Project.

References

Armour, K. C., C. M. Bitz, L. Thompson, and E. C. Hunke (2011), Controls on Arctic sea ice from first-year and multiyear ice survivability, *J. Clim.*, *24*(9), 2378–2390.

Blazey, B., M. Holland, and E. Hunke (2013), Arctic Ocean sea ice snow depth evaluation and bias sensitivity in CCSM, *The Cryosphere*, *7*(6), 1887–1900.

Hezel, P., X. Zhang, C. Bitz, B. Kelly, and F. Massonnet (2012), Projected decline in spring snow depth on Arctic sea ice caused by progressively later autumn open ocean freeze-up this century, *Geophys. Res. Lett.*, *39*, L17505, doi:10.1029/2012GL052794.

Hunke, E. C., W. H. Lipscomb, and A. K. Turner (2010), CICE: The Los Alamos sea ice model Documentation and Software User's Manual, version 4.1 LA-CC-06-012, T-3 Fluid Dynamics Group, Los Alamos National Laboratory.

Jahn, A., K. Sterling, M. M. Holland, J. E. Kay, J. A. Maslanik, C. M. Bitz, D. A. Bailey, J. Stroeve, E. C. Hunke, W. H. Lipscomb, et al. (2012), Late-twentieth-century simulation of Arctic sea ice and ocean properties in the CCSM4, *J. Clim.*, *25*(5), 1431–1452.

Kay, J. et al. (2014), The Community Earth System Model (CESM) large ensemble project: A community resource for studying climate change in the presence of internal climate variability, *Bull. Am. Meteorol. Soc.*, *96*, 1333–1349.

Kurtz, N. T., and S. L. Farrell (2011), Large-scale surveys of snow depth on Arctic sea ice from Operation IceBridge, *Geophys. Res. Lett.*, *38*, L20505, doi:10.1029/2011GL049216.

Kwok, R., and C. Haas (2015), Effects of radar side-lobes on snow depth retrievals from operation IceBridge, *J. Glaciol.*, *61*(227), 576–584.

Kwok, R., and D. Rothrock (2009), Decline in Arctic sea ice thickness from submarine and ICESat records: 1958–2008, *Geophys. Res. Lett.*, *36*, L15501, doi:10.1029/2009GL039035.

Light, B., S. Dickinson, D. K. Perovich, and M. M. Holland (2015), Evolution of summer Arctic sea ice albedo in CCSM4 simulations: Episodic summer snowfall and frozen summers, *J. Geophys. Res. Oceans*, *120*(1), 284–303, doi:10.1002/2014JC010149.

Lindsay, R. (1998), Temporal variability of the energy balance of thick Arctic pack ice, *J. Clim.*, *11*(3), 313–333.

Maslanik, J., J. Stroeve, C. Fowler, and W. Emery (2011), Distribution and trends in Arctic sea ice age through spring 2011, *Geophys. Res. Lett.*, *38*, L13502, doi:10.1029/2011GL047735.

Maslanik, J. A., C. Fowler, J. Stroeve, S. Drobot, J. Zwally, D. Yi, and W. Emery (2007), A younger, thinner Arctic ice cover: Increased potential for rapid, extensive sea ice loss, *Geophys. Res. Lett.*, *34*(17), doi:10.1029/2007GL032043.

Maykut, G. A., and N. Untersteiner (1971), Some results from a time-dependent thermodynamic model of sea ice, *J. Geophys. Res.*, *76*(6), 1550–1575, doi:10.1029/JC076i006p01550.

Nansen, F. (1905), *The Norwegian North Polar Expedition, 1893–1896: Scientific Results*, vol. 6, Green and Company, Longmans.

Newman, T., S. L. Farrell, J. Richter-Menge, L. N. Connor, N. T. Kurtz, B. C. Elder, and D. McAdoo (2014), Assessment of radar-derived snow depth over Arctic sea ice, *J. Geophys. Res. Oceans*, *119*, 8578–8602, doi:10.1002/2014JC010284.

Polashenski, C., D. Perovich, and Z. Courville (2012), The mechanisms of sea ice melt pond formation and evolution, *J. Geophys. Res.*, *117*, C1001, doi:10.1029/2011JC007231.

Serreze, M. C., M. M. Holland, and J. Stroeve (2007), Perspectives on the Arctic's shrinking sea-ice cover, *Science*, *315*(5818), 1533–1536.

Warren, S. G., I. G. Rigor, N. Untersteiner, V. F. Radionov, N. N. Bryazgin, Y. I. Aleksandrov, and R. Colony (1999), Snow depth on Arctic sea ice, *J. Clim.*, *12*(6), 1814–1829.

Webster, M. A., I. G. Rigor, S. V. Nghiem, N. T. Kurtz, S. L. Farrell, D. K. Perovich, and M. Sturm (2014), Interdecadal changes in snow depth on Arctic sea ice, *J. Geophys. Res. Oceans*, *119*, 5395–5406, doi:10.1002/2014JC009985.